CFD Simulation for Internal Flow in a Pipe – FDM and LBM

Bhavin Yardi
G.W. Woodruff School of Mechanical Engineering
Dr. Alexander Alexeev
December 12, 2024

This study compares two numerical methods, Finite Difference Method (FDM) and Lattice Boltzmann Method (LBM), for simulating internal fluid flow within a pipe. The analysis focuses on computational efficiency, accuracy, and the physical insights offered by each method across varying Reynolds numbers (Re = 100, 400, 2000). A structured computational domain and boundary conditions were established to ensure consistency in results. U-velocity profiles and spatial convergence rates were evaluated to validate numerical accuracy. The results show that while FDM provides higher spatial convergence, LBM is significantly faster, requiring only 89.59s compared to FDM's 252.83s runtime. However, LBM's stability is sensitive to mesh refinement and relaxation parameter adjustments. The findings highlight the trade-offs between these methods, with LBM excelling in computational efficiency and FDM offering greater reliability under less stringent stability conditions. These insights are valuable for optimizing numerical approaches in fluid mechanics applications.

Nomenclature

u = x-velocity of fluid
v = y-velocity of fluid
u^* = projected x-velocity
v^* = projected y-velocity
p = pressure of fluid
Δt = time step
Δx = grid size in x-direction
Δy = grid size in y-direction
i = iteration in x-direction
j = iteration in y-direction
U_o = free Stream velocity in x-direction
f_i = distribution in i-direction
c_{ia} = velocity of i^{th} distribution in x-direction
c_{ib} = velocity of i^{th} distribution in y-direction
c_s = velocity of sound
ρ = density of fluid
τ = relaxation parameter
D_h = hydraulic diameter of the pipe
μ = dynamic viscosity of the fluid

I. Introduction

The study of internal fluid flow is crucial across a wide range of engineering and industrial applications, such as pipeline transport, HVAC systems, heat exchangers, and automotive cooling systems. Internal flow is defined as fluid motion confined within solid boundaries, typically governed by the Navier-Stokes equations. The ability to accurately model and optimize internal flow is instrumental in improving energy efficiency, reducing operational costs, and enhancing system reliability. For example, in oil and gas pipelines, pressure drop prediction directly impacts energy consumption, while in HVAC systems, flow uniformity ensures thermal comfort and system longevity [1].

CFD (Computational Fluid Dynamics) is a powerful tool for analyzing internal flow in pipes [2] by simulating the behavior of fluids under various conditions. It provides detailed insights into key parameters like velocity profiles, pressure drops, flow patterns and effect of viscosity [3], which are critical for optimizing pipeline designs and ensuring efficient operation. By solving the Navier-Stokes equations numerically, CFD enables engineers to visualize flow characteristics, detect issues like turbulence or flow separation, and evaluate the effects of different geometries, boundary conditions, and Reynolds numbers. This capability is especially important in industries like oil and gas, HVAC, and chemical processing, where accurate predictions of internal flow can reduce energy costs, enhance system performance, and prevent failures.

In computational fluid dynamics (CFD), numerical methods like the Finite Difference Method (FDM) [4] and the Lattice Boltzmann Method (LBM) [5] are widely employed to simulate fluid flow. Both methods aim to solve the governing equations of fluid mechanics, yet they differ significantly in their underlying principles, computational frameworks, and applications. FDM is a

traditional approach that solves discretized versions of the Navier-Stokes equations using finite grid points. It is known for its robustness and accuracy but often requires significant computational resources for large-scale or complex geometries. On the other hand, LBM is a macroscopic method that models fluid flow based on particle distribution functions, making it computationally efficient and well-suited for simulating complex boundaries and multi-phase flows.

This project seeks to compare the performance of FDM and LBM for simulating internal flow in a pipe at various Reynolds numbers (Re = 100, 400, and 2000). The objectives include evaluating the accuracy, computational efficiency, and physical insights provided by both methods. Boundary conditions and domain setup are tailored to ensure consistency and comparability. By analyzing velocity profiles, spatial convergence rates, and runtime, this study aims to determine the suitability of these methods for specific fluid flow problems.

The motivation for this comparative study stems from the increasing demand for efficient numerical methods in CFD. While traditional methods like FDM have been extensively validated in literature, newer methods such as LBM are gaining traction due to their computational speed and scalability. Understanding the trade-offs between these methods can guide engineers in selecting the optimal approach for their specific applications, whether it be the precise modeling of low-Reynolds-number flows or computationally demanding high-Reynolds-number scenarios.

The outcomes of this study have implications for various industries, including automotive, aerospace, and energy, where internal flow optimization is a critical design parameter. Furthermore, this project contributes to the ongoing research in CFD by providing a detailed comparison of numerical techniques, paving the way for future advancements in fluid mechanics modeling.

II. Methodology

A. Domain, Boundary Conditions and Governing Equations

The computational domain represents the region of interest where the fluid flow is simulated. In this project, the domain is a rectangular pipe with a length of 1 meter and a height of 0.2 meters as shown in Fig.I. The rectangular grid is chosen instead of a square grid in order to reduce the height of the domain. This is done so that the effect of the walls can be seen on the fluid flow. The domain is discretized into a grid with grid spacing $\Delta x=\Delta y=0.01$m, resulting in 100 nodes along the x-direction and 20 nodes along the y-direction. This choice of domain size and grid resolution ensures sufficient accuracy while balancing computational efficiency.

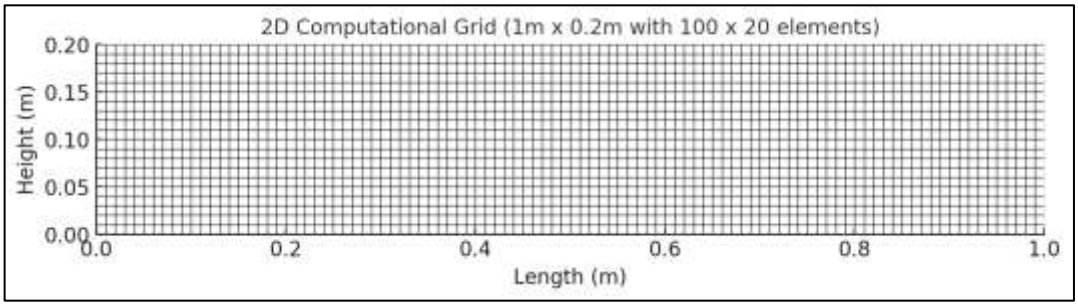

Fig.I. Domain for Simulation

Boundary conditions are essential for accurately modeling fluid flow and ensuring stability in numerical simulations. In this case, several key boundary conditions are applied:

i) **Inlet Boundary Condition**: At the inlet (left boundary), a velocity profile is imposed. For simplicity, we assume a uniform velocity distribution at the entrance of the pipe. This free stream velocity is taken to be 1m/s. No penetration is assumed at the inlet, hence the y-component of velocity is assumed to be 0m/s. The fluid is assumed to enter the domain with a specified velocity profile, which is critical for accurately predicting flow patterns downstream. The pressure is taken to be ambient (1atm) at the inlet.

ii) **Outlet Boundary Condition**: At the outlet (right boundary), a gradient boundary condition is applied, where the gradient of the pressure, x-velocity and y-velocity is considered to be 0, and the flow is assumed to exit the domain freely. This condition helps in capturing the behavior of the flow as it exits the pipe and ensures proper mass conservation.

iii) **Wall Boundary Condition**: The walls of the pipe (top and bottom boundary) are treated as solid boundaries, where the velocity of the fluid is assumed to be zero at the boundary (no-slip condition). This is modeled using the bounce-back boundary condition in LBM, where distribution functions are reflected back along the boundary, enforcing the no-slip condition. For pressure, an ambient pressure (1atm) is applied on both of these boundaries.

These boundary conditions summarized in Fig.II, together with the choice of domain and grid resolution, are key to the accuracy and stability of the simulation. Proper handling of the boundary conditions is vital in ensuring the realistic representation of fluid dynamics, especially in simulating flow features such as velocity profiles, turbulence, and pressure drops.

Physical Parameter	Top Boundary	Bottom Boundary	Left Boundary	Right Boundary
Pressure	Ambient	Ambient	Ambient	Gradient
X-Velocity	Wall	Wall	Ambient	Gradient
Y-Velocity	Wall	Wall	Wall	Gradient

Fig. II. Boundary Conditions

For the flow, the governing transient, incompressible and dimensionless form of Navier-Stokes Equation is given by:

i) Equation of Continuity: $\frac{\partial u}{\partial x} + \frac{\partial v}{\partial y} = 0$

ii) X-momentum Equation: $\frac{\partial u}{\partial t} + u\frac{\partial u}{\partial x} + v\frac{\partial u}{\partial y} = -\frac{\partial p}{\partial x} + \frac{1}{Re}\left(\frac{\partial^2 u}{\partial x^2} + \frac{\partial^2 u}{\partial y^2}\right)$

iii) Y-momentum Equation: $\frac{\partial v}{\partial t} + u\frac{\partial v}{\partial x} + v\frac{\partial v}{\partial y} = -\frac{\partial p}{\partial y} + \frac{1}{Re}\left(\frac{\partial^2 v}{\partial x^2} + \frac{\partial^2 v}{\partial y^2}\right)$

Where, Reynold's Number (Re) = $\frac{\rho * D_h * U_o}{\mu}$

B. Finite Difference Method

For this project, the FDM is solved using the explicit approach, where the X-momentum and Y-momentum are coupled with the Pressure Poisson's Equation. The SOR method is used to solve the Pressure Poisson's Equation. The equations have been discretized using the central difference scheme in the following manner:

i) X-Momentum: $u^* = u^n + \Delta t^*\left(-\frac{\partial u^2}{\partial x} - \frac{\partial uv}{\partial y} + \frac{1}{Re}\left(\frac{\partial^2 u}{\partial x^2} + \frac{\partial^2 u}{\partial y^2}\right)\right)$

$$\frac{\partial u^2}{\partial x} = \frac{0.5*\left(u_{(i,j)}+u_{(i,j+1)}\right)^2 - 0.5*\left(u_{(i,j)}+u_{(i,j-1)}\right)^2}{\Delta x}$$

$$\frac{\partial uv}{\partial y} = \frac{\left(0.5*\left(u_{(i,j)}+u_{(i-1,j)}\right)*0.5*\left(v_{(i-1,j)}+v_{(i-1,j+1)}\right)\right) - \left(0.5*\left(u_{(i,j)}+u_{(i+1,j)}\right)*0.5*\left(v_{(i,j)}+v_{(i,j+1)}\right)\right)}{\Delta y}$$

$$\frac{\partial^2 u}{\partial x^2} + \frac{\partial^2 u}{\partial y^2} = \frac{u_{(i,j+1)} - 2u_{(i,j)} + u_{(i,j-1)}}{\Delta x^2} + \frac{u_{(i+1,j)} - 2u_{(i,j)} + u_{(i-1,j)}}{\Delta y^2}$$

ii) Y-Momentum: $v^* = v^n + \Delta t\left(-\frac{\partial v^2}{\partial y} - \frac{\partial uv}{\partial x} + \frac{1}{Re}\left(\frac{\partial^2 v}{\partial x^2} + \frac{\partial^2 v}{\partial y^2}\right)\right)$

$$\frac{\partial v^2}{\partial y} = \frac{0.5*\left(v_{(i,j)}+v_{(i-1,j)}\right)^2 - 0.5*\left(v_{(i,j)}+v_{(i+1,j)}\right)^2}{\Delta y}$$

$$\frac{\partial uv}{\partial x} = \frac{\left(0.5*\left(u_{(i,j)}+u_{(i+1,j)}\right)*0.5*\left(v_{(i,j)}+v_{(i-1,j+1)}\right)\right) - \left(0.5*\left(u_{(i,j)}+u_{(i+1,j-1)}\right)*0.5*\left(v_{(i,j)}+v_{(i,j-1)}\right)\right)}{\Delta y}$$

$$\frac{\partial^2 v}{\partial x^2} + \frac{\partial^2 v}{\partial y^2} = \frac{v_{(i+1,j)} - 2v_{(i,j)} + v_{(i-1,j)}}{\Delta x^2} + \frac{v_{(i,j+1)} - 2v_{(i,j)} + v_{(i,j-1)}}{\Delta y^2}$$

iii) Pressure Poisson's Equation: $\frac{\partial^2 p}{\partial x^2} + \frac{\partial^2 p}{\partial y^2} = \frac{1}{\Delta t}\left(\frac{\partial u^*}{\partial x} + \frac{\partial v^*}{\partial y}\right)$

$$\frac{\partial^2 p}{\partial x^2} + \frac{\partial^2 p}{\partial y^2} = \frac{p_{(i+1,j)} - 2p_{(i,j)} + p_{(i-1,j)}}{\Delta x^2} + \frac{p_{(i,j+1)} - 2p_{(i,j)} + p_{(i,j-1)}}{\Delta y^2}$$

$$\frac{\partial u^*}{\partial x} + \frac{\partial v^*}{\partial y} = \frac{u^*_{(i,j+1)} - u^*_{(i,j-1)}}{2\Delta x} + \frac{v^*_{(i+1,j)} - v^*_{(i-1,j)}}{2\Delta y}$$

iv) Updating Velocities:

$$u^{n+1} = u^* - \Delta t\frac{\partial p}{\partial t}$$

$$v^{n+1} = v^* - \Delta t\frac{\partial p}{\partial t}$$

The domain for solving FDM, as shown in Fig.III, consists of ghost nodes for pressure in both x-directions and y-directions. For x-velocities, there are ghost nodes only in the y-direction and only in the x-direction for y-velocities. The boundary conditions are applied on each of the boundaries w.r.t these ghost nodes. The final x-velocities and y-velocities are calculated by averaging across all the intermediate nodes. The solver parameters are kept as the following:

Grid Size = 0.01 x 0.01m | Δt = 0.001s | Re: 100, 400, 2000 | U^o = 1m/s

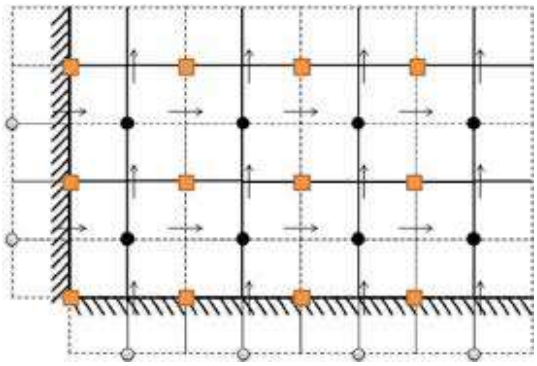

Fig. III. Staggered Grid with Ghost Nodes

C. Lattice Boltzmann Method

The D2Q9 lattice, shown in Fig.IV, is used to solve the Lattice Boltzmann Method. The method starts with the collision step and then has the propogation step. The half-way bounce back is used to compute the macroscopic velocities at the boundaries.

The following algorithm is used to compute the velocities:

i) Weight allocation: Initial Weights are allocated to the distributions –

$a_0 = 4/9$ | $a^1 = a^2 = a^3 = a^4 = 1/9$ | $a^5 = a^6 = a^7 = a^8 = 1/36$

ii) Density and Macroscopic Velocity Calculation:

$$\rho = \sum a_i$$

$$u = \frac{\sum a_i * c_a}{\rho}$$

$$v = \frac{\sum a_i * c_b}{\rho}$$

iii) Collision Step:

$$f_i^*_{(i,j)} = f_{i(i,j)} + \Delta f_{i(i,j)}$$

$$\Delta f_{i(i,j)} = -\frac{1}{\tau}(f_{i(i,j)} - f^{eq}{}_{i(i,j)}$$

$$f^{eq}{}_{i(i,j)} = a_i \rho(1 + \frac{c_{ia} * u_a}{c^2{}_s} + \frac{Q_{iab} * U_a * U_b}{2 * C^4{}_s}$$

$$Q_{iab} = C_{ia} * C_{ib} - C^2{}_s \delta_{ab}$$

iv) Streaming Step

a) At all internal Nodes: $f_{i(x + ci,\, t+1)} = f^*_{i(x,t)}$

b) For Moving Wall: $f_{i(x,\, t+1)} = f'_{i(x,t)} - \frac{2 a_i \rho u_a c_{ia}}{c^2{}_s}$

c) For Stationary Wall: $f_{i(x,\, t+1)} = f'_{i(x,t)}$

The solver parameters are kept as the following:

$\Delta x = \Delta y = \Delta t = 1$ | $c_s = \frac{1}{\sqrt{3}}$ | $U_o = 0.1$

For ensuring the stability of the LBM, the value of τ is kept greater than 0.6, and the value of $\frac{U_o}{C_s}$ is always kept to be less than 0.1. Also, for performing all the post processing and comparison the value of $\frac{u}{U_o}$ and $\frac{v}{U_o}$ is calculated and plotted.

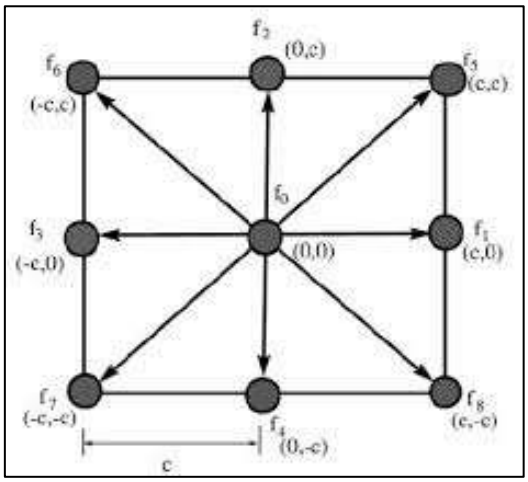

Fig. IV D2Q9 Lattice

III. RESULTS

Based on the 2 solvers, domain and the boundary conditions, we run the simulation till steady state. The steady state tolerance is kept to be 10^{-6}. On achieving the steady state, we plot the x-velocity contours and the centerline velocities, to obtain the following results:

i) Fig.V. (a), (b) & (c) show the x-velocity contour for the Re: 100, 400 and 2000. From the contours, we can clearly see the developing boundary layer. Also, from the graphs, we can see that as the Reynold's Number increases, the boundary layer thickness decreases. Also, we can see that there are some disturbances in the contour of Re:2000, this can be attributed to the fact that Re:2000 is close to the transition Reynold's number of 2300 for a closed pipe. And, this closeness to turbulent flow gives rise to these disturbances, which in other low Reynolds's number cease to exist.

ii) Fig. VI. Shows the centerline comparison for the x-velocities. From this graph, we can clearly validate the principles of Fluid Mechanics, which state that as the Reynolds's Number increases, the boundary layer thickness decreases. Also, we can see that there is a clear parabolic profile for Re:100, but there appears to be flattened profile for Re:400 and Re:2000. This can be attributed to the fact, that as the Reynold's number increases, the boundary layer thickness decreases and the effect of the walls also decreases. Due to this decreased impact of the wall, a decreased fraction of cross-section experiences velocities less than $U_{o,}$ which gives rise to the flattened section. Also, here we can see that there is a part of the cross section, where the x-velocity goes beyond the value of U_o. This happens because when there is the section which is a part of the boundary layer whose x-velocities are below $\underline{U_o}$, there has to be a cross-section, whose x-velocities surpass U_o, so that the mass flowing through every cross-section in the pipe can be conserved. Also, there is an asymmetrical centerline profile that is seen for Re:2000. The reason for this profile was not found during this study. This might be due to the transition Reynold's number, but the exact reason is yet to be found.

iii) Fig. VII shows the comparison of centerline velocity for Re: 400, obtained through FDM, LBM and through simulation on ANSYS Fluent. Simulation was performed on ANSYS Fluent to attain a baseline comparison for the other two methods. On comparison, it can be seen that the LBM matches very closely with the profile from ANSYS Fluent. The FDM predicts a similar boundary layer thickness as the other 2 methods, but the net x-velocity profile doesn't match very accurately with the other methods.

iv) The runtimes of the 2 methods: LBM and FDM were recorded for a Re: 400. It was seen that LBM took 89.59s to simulate, whereas the FDM took 252.83s to simulate. As expected, the LBM is much faster than FDM.

v) The Spatial Convergence Rate was also calculated for the 2 methods. The Spatial Convergence Rate for FDM was obtained to be 1.78, which is close to 2. In FDM, we expect the Spatial Convergence Rate to be 2, because of the Central Difference Scheme used. The Spatial Convergence Rate for the LBM is obtained to be 1.1868.

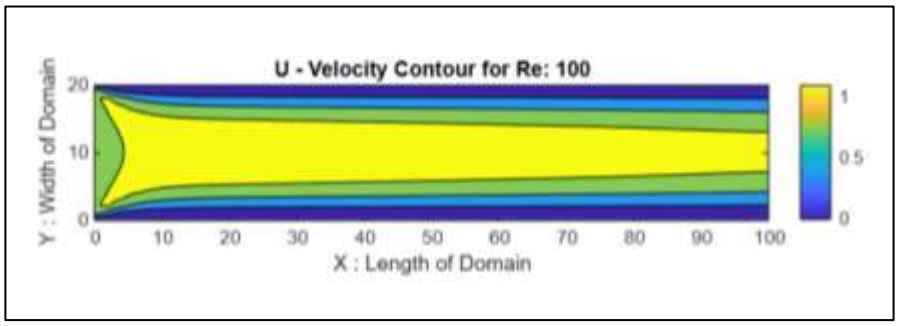

Fig.V. (a) X-velocity contour for Re: 100

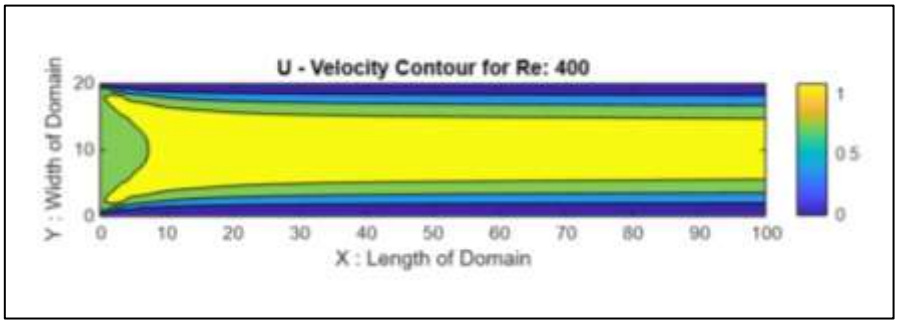

Fig.V. (b) X-Velocity Contour for Re: 400

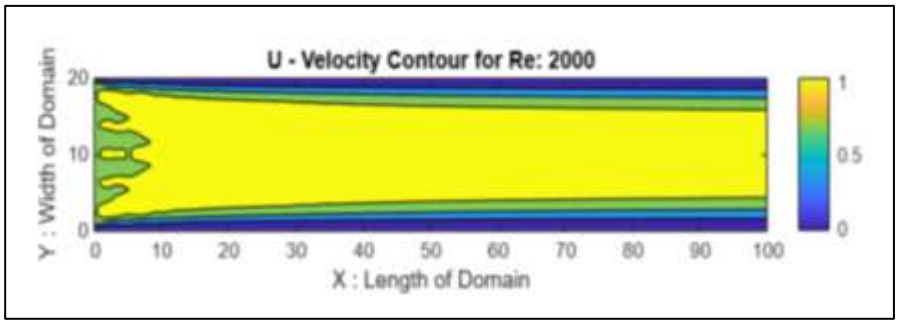

Fig.V. (c) X-Velocity Contour for Re: 2000

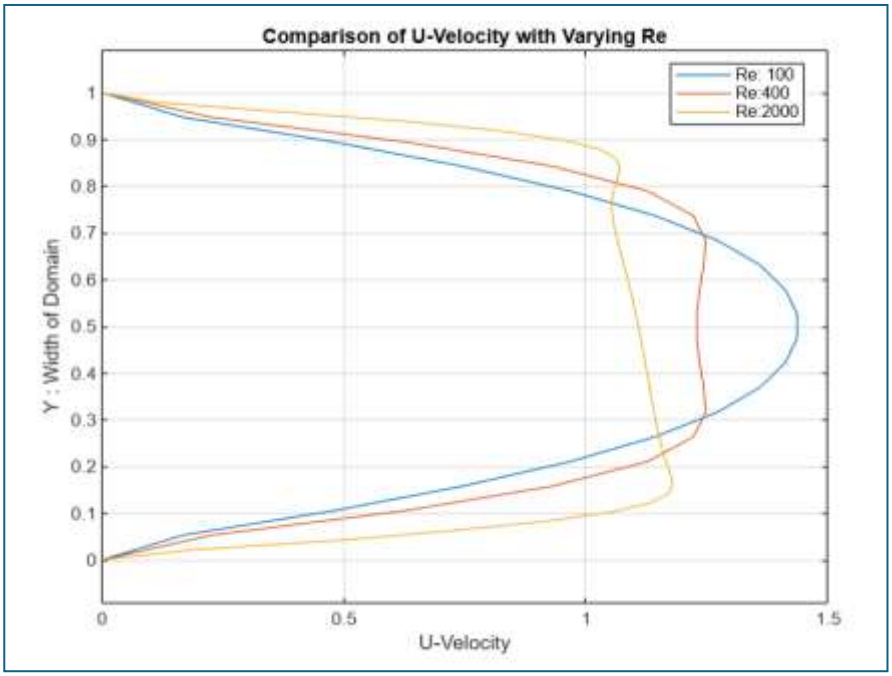

Fig.VI.. Comparing centerline velocity for Re: 100, 400 and 2000

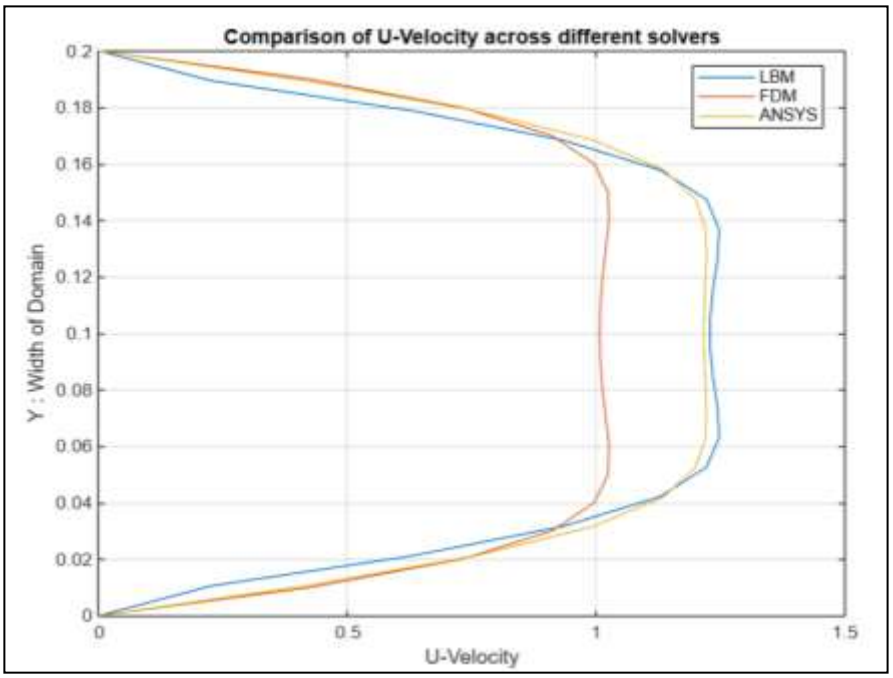

Fig.VII Comparing the centerline velocity for Re: 400 across FDM, LBM and ANSYS Fluent

IV. CONCLUSION

From the above results, the following conclusions can be drawn:

i) From the runtimes of the two methods, it can be seen that LBM is a much faster method as compared to FDM, making it a much more computationally efficient method as compared to the FDM.

ii) While running the LBM, a lot of care must be taken to keep the relaxation parameter (τ), and the $\frac{U_o}{C_s}$ within its stability criteria, else the LBM becomes unstable, and gives a value of 'NaN' for all velocities at all grid points.

iii) While iterating through different boundary conditions for the given domain and physical setup it was found that solutions are very sensitive to the accurate boundary conditions for the x-velocities and y-velocities. For Pressure, it is only the outlet Pressure boundary condition that affects the solution. The pressure for the other boundaries is implicitly always calculated through the projected velocities.

iv) The x-velocity shoots up to values greater than 1 at fractions of the cross-section outside the boundary layer, to conserve mass at all cross-sections.

v) For both the solvers, comparing the BL thickness, across different Re, we can see that the results follow the principles of Fluid Mechanics, which the BL thickness decreases as Re increases, thus validating the results.

The comparison between the Finite Difference Method (FDM) and the Lattice Boltzmann Method (LBM) was successful in evaluating the strengths and limitations of each approach for simulating internal fluid flow. The study highlighted FDM's robustness and higher spatial convergence rates, making it a reliable method for problems requiring high accuracy. On the other hand, LBM demonstrated superior computational efficiency, achieving faster runtimes and handling complex boundary conditions effectively. The analysis also revealed that while FDM offered greater stability under broader conditions, LBM required careful tuning of parameters like the relaxation time to maintain stability. Overall, the findings provide valuable insights into the trade-offs between accuracy, stability, robustness, and computational efficiency, helping guide the choice of numerical methods for specific fluid dynamics application.

V. REFERENCES

[1] Kirkpatrick, Allan T. "Fluid Flow in Refrigeration and Air Conditioning Systems." Introduction to Refrigeration and Air Conditioning Systems: Theory and Applications. Cham: Springer International Publishing, 2022. 65-89.

[2] Lamsal, Abish. "Analyzing pipe flow scenarios using computational fluid dynamics (CFD)." Int. J. Eng. Appl. Sci. Technol 8.3 (2023): 162-166.

[3] Debtera, Baru, Venkatesa Prabhu Sundramurthy, and Ibsa Neme. "Computational fluid dynamics simulation and analysis of fluid flow in pipe: Effect of fluid viscosity." Journal of Computational and Theoretical Nanoscience 18.3 (2021): 805-810.

[4] Srivastava, Mohit Kumar, Love Trivedi, and Rakshit Kaushik. "Investigation of 2-dimensional fluid flow using finite difference flow method of Navier-Stokes equation." arXiv preprint arXiv:2209.02059 (2022).

[5] Zhao, Huizhe, Aydin Nabovati, and Cristina H. Amon. "Analysis of Fluid Flow in Porous Media Using the Lattice Boltzmann Method: Inertial Flow Regime." Fluids Engineering Division Summer Meeting. Vol. 44755. American Society of Mechanical Engineers, 2012.